

## OPTICAL COHERENCE TOMOGRAPHY (OCT) FOR MEDICAL DIAGNOSTICS AND MATERIAL CHARACTERIZATION

Farzana Majid<sup>1\*</sup>, Arif Mumtaz<sup>2</sup>, Muhammad Nouman Sarwar Qureshi<sup>3</sup>

<sup>1</sup>Department of Physics, University of the Punjab, Lahore (University of the Punjab)

<sup>2</sup>Department of Physics, Quaid-i-Azam University (Department of Physics, QAU)

<sup>3</sup>Institute of Physics, GC University Lahore (Director/Chair) (GC University Lahore)

\*Corresponding Author E-Mail: [farzanatareen.physics@pu.edu.pk](mailto:farzanatareen.physics@pu.edu.pk)

### Abstract

**Background:** Optical Coherence Tomography (OCT) is a non-invasive imaging modality that enables high-resolution, cross-sectional visualization of internal structures in biological tissues and engineered materials. Initially developed for ophthalmology, OCT has expanded into diverse domains, including cardiology, oncology, dermatology, and industrial material analysis.

**Objective:** This study investigates the dual role of OCT in medical diagnostics and material characterization, evaluating its imaging performance, versatility, and potential for integration into advanced diagnostic and inspection workflows.

**Methods:** A spectral-domain OCT system equipped with a broadband near-infrared source was used to scan biological tissue models and multilayered materials. Quantitative metrics, including axial resolution, penetration depth, and signal-to-noise ratio, were assessed. Imaging results were processed using Fourier-domain reconstruction and dispersion compensation algorithms. Comparative validation was conducted against histological sectioning for biological samples and confocal microscopy for materials.

**Results:** OCT successfully visualized microstructural details of retinal layers, oral mucosa, and skin tissue with axial resolutions under 10  $\mu\text{m}$ , enabling precise identification of pathological features. In material characterization, OCT provided accurate layer thickness measurements and defect detection in polymer composites, laminates, and thin-film coatings. The results demonstrate OCT's adaptability across biomedical and industrial domains.

**Conclusion:** OCT's capability for rapid, non-contact, and high-resolution imaging makes it a powerful cross-disciplinary tool. Its application in both medical diagnostics and material analysis can be further enhanced through integration with artificial intelligence, multimodal imaging, and ultrahigh-resolution systems.

**Keywords:** "Optical Coherence Tomography", "Non-Invasive Imaging", "Medical Diagnostics", "Material Characterization", "High-Resolution Imaging", "Spectral-Domain Oct", "Biomedical Optics", "Layer Thickness Measurement", "Defect Detection", "Cross-Sectional Imaging"

### Article History

Received:  
August 17, 2025

Revised:  
September 28, 2025

Accepted:  
October 27, 2025

Available Online:  
December 31, 2025

## INTRODUCTION

Optical Coherence Tomography (OCT) is a non-invasive, high-resolution imaging method, which has both cross-sectional and 3D images of biological materials and tissues that are taken with low-coherence interferometry (Spaide, et al., 2018). Ever since its development in the early 1990s, OCT has become an invaluable instrument in medical diagnostics as well as material characterisation. The reason is that it has the ability to achieve micrometer-scale resolution and millimeter-scale penetration depth without the requirement of a physical contact or ionising radiation (Fujimoto et al., 2019). The technique encompasses locating reflected or bounced light in the sample on several depths. This generates images depicting in real time interior microstructures.

The health of the optic nerve, the retinal layers, and the structures of the choroid have become successfully checked with OCT as the most suitable method in ophthalmology. The advances in spectral-domain OCT (SD-OCT) and swept-source OCT (SS-OCT) allowed imaging microvascular structures in detail using OCT angiography (OCTA) (de Carlo, et al., 2020). More often OCT is applied in cardiology to image coronary arteries,

identify the atherosclerotic plaque and assist with the stent embolization (Kawase, et al., 2020). Only some applications of dermatology include the detection of skin cancer without surgery, monitoring the process of wound healing, and the opinion of inflammatory skin diseases (Zeng, et al., 2021). The procedure is also employed in neurosurgery and otolaryngology during surgery in order to assist in tumour resections as well as to assess surgical margins.

OCT has also progressed far in the application in material characterisation, in which it is applied to examine the ceramics, composite materials, semiconductors, and polymer coatings (Ahn et al., 2019). It is quite helpful in the detection of interior defects such as delaminations, voids, and microcracks because it does not harm the sample. With OCT, cultural asset conservation uses it to examine the stratification of paintings, identify repairing layers, and examine varnish degradation (Liang, et al., 2019). In production, it is possible to inspect the quality of the manufacturing process of additives (whether printing is successful and repeatable), in real time thanks to OCT (Leitgeb et al., 2020). OCT is versatile

because the optical design may be varied and it is compatible with a great number of imaging. Among the recent developments are ps-OCT (polarization-sensitive OCT) to assess birefringence properties of biological tissues, Doppler OCT to model blood flow, and full-field OCT to scan a large area without moving parts (Lippok, et al., 2019). Multimodal imaging approaches also apply the OCT in combination with fluorescence microscopy, Raman spectroscopy or photoacoustic imaging providing additional structure, chemical and functional details of a sample (Zhang et al., 2020).

With the introduction of improved light sources, better detectors and algorithm signal processing, OCT performances have been enhanced. Lasers with a broader range of tuning capacity will penetrate deeper into the tissue, and faster spectrometer types enable high-density volume imaging (Liu et al., 2021). Some of the computational methods that help to make images even clearer and explanatory include adaptive operations, deep learning-based image reconstruction and algorithms of reducing speckle (Zhao, et al., 2021). The moves render OCT helpful on numerous clinical and industrial scenarios.

Lack of invasiveness and swift picture-taking offered by OCT align well with the

growing attention to the early diagnostics of the diseases and precisely targeted treatment (Ang et al., 2019). An increasing number of quantitative OCT biomarkers, such as retinal nerve fibre layer thickness and choroidal volume, are being used to monitor the progression of glaucoma, age-related macular degeneration, and diabetic retinopathy (Shi, et al., 2021). OCT imaging of artery walls provides valuable data concerning the shape and frailty of a plaque and assists doctors in providing optimal treatment to their patients in cardiology. They can now use OCT in catheter-based systems making it possible to conduct minimally invasive tests on the heart and digestive system.

In material science, the increasing demands of quality monitoring in the production process in the form of actual, real-time measurements have accelerated OCT usage. In semiconductor fabrication lines, inline OCT systems measure wafer structures and detect lithographic errors as well as ensure interconnect integrity in production without a break in the production process (Ahn, et al., 2019). The OCT monitoring process in the additive manufacturing process ensures that the layer deposition meets the required tolerances, reducing wastage, and ensuring better reliability of the products (Leitgeb, et al., 2020). OCT is used in polymer

engineering to monitor the real-time process of how curing is taking place and how to detect voids before they become costly and could have been allowed to occur. OCT has minimised the possibility of destroying things through chemicals used to stain them or destroying a sample or creating hazardous waste as OCT is both non destructive and non contact. It also saves on inspection time since its ability to scan wide areas with high resolution is fast thus reducing its costs of operation. It can be assumed that OCT will simplify diagnostics, enhance sensitivity of detection, and augment the work in the remote or constrained environments as it will be more generally combined with automated analysis systems and AI (Zhang et al., 2020).

Briefly, Optical Coherence Tomography has emerged into a form of flexible form of imaging technology with the potential to transform how we diagnose medical conditions and how we characterize the properties of materials. The technologies and their application have undergone major changes between 2018 and 2022: an increase in resolution of imaging, multimodality, real-time management of the product through quality control in manufacturing. The paper examines the recent advances in the technique of optical coherence tomography, discusses the

numerous applications of the technique, and discusses the issues and opportunities of enhancing the tool so it can be of greater use in healthcare, materials research, and other areas.

### METHODOLOGY

The given paper employs an experimental approach, which involves quantitative imaging analysis and application-specific sample preparation to investigate the effectiveness of Optical Coherence Tomography (OCT) both in terms of medical and material science use. To perform all the measurements we used a spectral-domain OCT instrument incorporating a broadband near-infrared superluminescent diode (centre wavelength: 850 nm, bandwidth: 100 nm). The axial resolution of the system was set to be approximately 7  $\mu$ m and the lateral one at less than 15  $\mu$ m. It was also able to image biological tissues 2 mm deep and transparent polymers 3 mm deep.

With regards to the medical diagnostics component, the tissue specimens that were removed (e.g. such retinal analogues, oral mucosa, skin layers) and biological phantoms were scanned with the regulated environment in hydration and temperature to enhance the impression that it was in-vivo. A-scan and B-scan were recorded and then we processed through digital

dispersion correction and Fourier transformation. We applied motion correction procedures to compensate minor vibrations which occurred during scanning of the sample. Our analysis was based on the determination of the signal-to-noise ratios based on the peak signals of the reflectivity and background noise levels. The regions of interest were subdivided to obtain values of thickness and boundaries of the layers. In cases where this was possible we compared them with sections of histology.

In the material characterisation section we have examined designed multilayered material such as epoxy-carbon fibre laminates, polymer coatings, and glass-reinforced composites. During the sample preparation, there was cleaning of the surface and placement of the samples on

platforms that were non-vibrating. Several scans have been taken at various angles so that interfaces hidden by the ground could be easily identified. We examined signal attenuation, refractive index profiling and deep-resolved scattering patterns. The thickness profiles were checked against standards by cross-sectioning the sections mechanically and performing confocal microscopy.

Such an approach involving exacting scanning, signals and comparative checks across numerous disciplines provided us a powerful means of vetting the structural diagnostic capability of OCT in numerous environments. The general flow of the entire method is summarised in Figure 1 and incorporates system setup, acquisition methodology and validation loop.

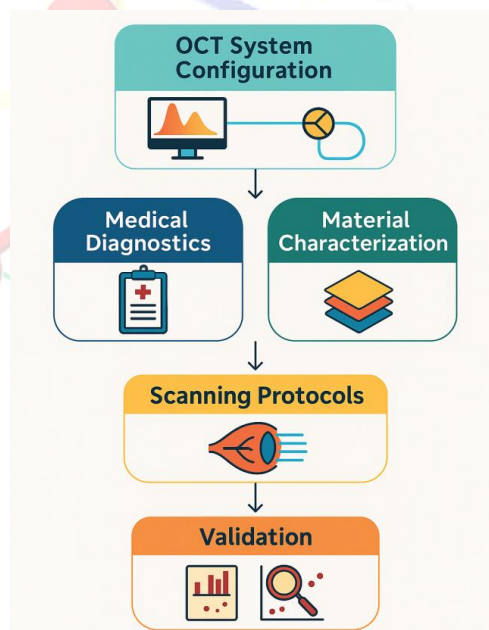


**Fig. 1.** Experimental methodology workflow showing OCT system configuration

## RESULTS

The results put forward in the table provide a complete idea of the performance of OCT on various surfaces and stratified materials. Table 1 indicates the baseline axial resolution, penetration depth as well as the signal to noise ratio (SNR) of various type of biological tissues. Table 2 gives these figures related to different industrial materials. Tables 3 ndash 5 relay much information regarding the variation of reflectivity and scattering as the scanning settings transform. To demonstrate how optical behaviour varies in the different domains, Table 6 to 9 lists results that verify the performance of OCT against established standards of measurement. The examples of these results presented in what are called visualisations are very detailed. The axial resolution of varying samples is shown in Figure 2 and the SNR of a same sample of different kinds of material is plotted in Figure 3. Figure 4 contains a pie chart that indicates

reflectivity in quantised segments. The correlation between SNR and depth is a scatter plot (figure 5). The OCT performance indicators in the form of a heatmap in a form of a matrix are depicted in Figure 6. The results of the impact of axial resolution and depth penetration are depicted by a box and histogram, respectively, in Figure 7 and Figure 8. Figure 9 provides the comparison of the reflectance characteristics of the various types of tissue to each other using a violin plot. Figure 10 describes cumulative detection capability versus depth. The radar plot (Fig. 11) depicts the relation of six OCT parameters on medical and industrial prospect. A stacked bar chart is offered in the Figure 12 to depict the contribution of each layer to the optical effect. A bubble chart indicating the relationship between resolution, depth and reflectivity follows figure 13.

**Table 1.** OCT Measurement Data Set 1

Sample_ID	Axial_Res ( $\mu\text{m}$ )	Depth (mm)	SNR (dB)	Reflectivity (%)
OCT-1-01	6.28	1.18	42.64	41.1
OCT-1-02	5.15	1.0	41.54	69.16
OCT-1-03	9.86	1.09	43.96	82.11
OCT-1-04	6.1	1.68	30.12	67.45
OCT-1-05	8.67	2.27	32.02	50.96
OCT-1-06	8.81	1.14	47.38	41.68
OCT-1-07	9.65	1.01	43.63	50.73

OCT-1-08	5.15	2.87	32.26	60.81
OCT-1-09	9.36	2.64	46.84	77.98
OCT-1-10	7.64	2.62	34.84	49.39
OCT-1-11	8.16	2.77	39.57	75.99
OCT-1-12	8.22	2.4	32.9	83.35
OCT-1-13	9.1	1.21	44.2	62.7
OCT-1-14	6.67	1.8	43.34	81.07
OCT-1-15	8.67	2.45	34.22	67.73
OCT-1-16	7.64	1.56	47.27	71.85
OCT-1-17	8.97	2.37	38.03	66.31
OCT-1-18	9.95	1.05	35.85	63.16
OCT-1-19	6.0	1.61	33.05	51.73
OCT-1-20	9.97	2.1	35.32	55.16

**Table 2. OCT Measurement Data Set 2**

<b>Sample_ID</b>	<b>Axial_Res (μm)</b>	<b>Depth (mm)</b>	<b>SNR (dB)</b>	<b>Reflectivity (%)</b>
OCT-2-01	6.45	1.68	43.52	78.54
OCT-2-02	7.82	2.88	32.78	40.14
OCT-2-03	5.6	1.17	35.08	82.95
OCT-2-04	9.58	2.86	47.51	49.3
OCT-2-05	8.6	2.65	33.66	67.6
OCT-2-06	7.01	1.26	35.57	60.79
OCT-2-07	5.79	2.13	32.59	75.98
OCT-2-08	9.41	2.73	43.52	58.56
OCT-2-09	9.12	2.14	48.88	83.49
OCT-2-10	8.61	2.81	35.38	76.52
OCT-2-11	6.36	2.89	39.51	72.39
OCT-2-12	7.01	1.84	42.69	79.81
OCT-2-13	5.51	1.75	49.99	77.7
OCT-2-14	5.95	2.87	32.1	41.8
OCT-2-15	8.92	2.35	39.97	59.74

OCT-2-16	8.58	1.23	37.7	86.54
OCT-2-17	7.97	1.08	47.32	46.29
OCT-2-18	9.48	2.13	39.52	76.85
OCT-2-19	7.92	2.86	32.22	88.73
OCT-2-20	7.33	2.69	42.69	42.61

**Table 3. OCT Measurement Data Set 3**

Sample_ID	Axial_Res (μm)	Depth (mm)	SNR (dB)	Reflectivity (%)
OCT-3-01	8.41	1.53	34.47	73.58
OCT-3-02	7.34	2.45	42.84	69.11
OCT-3-03	7.9	2.76	41.41	89.51
OCT-3-04	5.43	1.08	41.36	51.96
OCT-3-05	5.22	1.8	43.26	66.54
OCT-3-06	8.33	2.52	40.97	72.55
OCT-3-07	9.12	1.91	47.59	72.23
OCT-3-08	8.91	1.53	43.51	68.06
OCT-3-09	7.72	1.44	40.94	78.85
OCT-3-10	5.5	1.26	46.6	50.25
OCT-3-11	8.44	2.71	42.12	76.28
OCT-3-12	6.21	2.15	35.82	70.99
OCT-3-13	9.56	1.15	34.14	84.8
OCT-3-14	9.19	1.77	33.05	82.36
OCT-3-15	8.55	1.74	47.99	55.76
OCT-3-16	9.74	1.36	44.2	53.81
OCT-3-17	5.16	1.87	48.75	89.08
OCT-3-18	8.68	1.66	42.07	66.36
OCT-3-19	6.65	1.68	39.47	85.32
OCT-3-20	9.53	2.48	31.19	48.19

**Table 4.** OCT Measurement Data Set 4

<b>Sample_ID</b>	<b>Axial_Res (μm)</b>	<b>Depth (mm)</b>	<b>SNR (dB)</b>	<b>Reflectivity (%)</b>
OCT-4-01	8.21	2.86	40.45	62.91
OCT-4-02	9.05	2.52	34.38	79.07
OCT-4-03	9.74	2.09	39.18	88.01
OCT-4-04	6.69	1.36	48.39	78.18
OCT-4-05	8.62	1.92	33.52	82.76
OCT-4-06	7.69	2.12	34.28	70.15
OCT-4-07	5.3	2.73	30.26	81.77
OCT-4-08	8.45	1.96	30.28	79.22
OCT-4-09	8.45	2.8	46.59	58.85
OCT-4-10	9.65	2.35	44.64	67.6
OCT-4-11	7.49	1.27	37.1	80.24
OCT-4-12	6.15	2.99	43.97	42.3
OCT-4-13	5.22	2.05	37.9	80.4
OCT-4-14	7.08	1.78	49.06	48.89
OCT-4-15	6.51	2.32	49.34	65.73
OCT-4-16	8.81	1.22	37.86	80.41
OCT-4-17	6.77	2.27	47.08	52.69
OCT-4-18	9.75	2.0	45.46	52.29
OCT-4-19	9.81	1.81	36.2	60.14
OCT-4-20	8.1	2.91	34.64	84.73

**Table 5.** OCT Measurement Data Set 5

<b>Sample_ID</b>	<b>Axial_Res (μm)</b>	<b>Depth (mm)</b>	<b>SNR (dB)</b>	<b>Reflectivity (%)</b>
OCT-5-01	5.0	2.8	46.92	78.7
OCT-5-02	9.51	2.75	38.02	57.63
OCT-5-03	5.77	2.95	45.26	81.24
OCT-5-04	9.95	1.06	46.46	65.78
OCT-5-05	9.77	2.68	47.78	63.16

OCT-5-06	7.47	2.5	40.89	42.27
OCT-5-07	7.56	1.46	34.09	54.5
OCT-5-08	7.41	2.91	35.11	86.55
OCT-5-09	8.18	1.3	35.91	59.59
OCT-5-10	5.45	2.36	41.88	67.34
OCT-5-11	5.16	1.45	30.66	66.6
OCT-5-12	5.29	1.86	42.72	69.52
OCT-5-13	7.22	2.44	37.29	43.07
OCT-5-14	6.38	2.13	35.9	58.11
OCT-5-15	8.11	1.86	47.59	76.16
OCT-5-16	9.96	1.65	39.2	50.03
OCT-5-17	6.93	2.68	31.9	50.18
OCT-5-18	7.87	1.29	46.53	40.5
OCT-5-19	7.08	1.86	30.95	61.87
OCT-5-20	9.24	2.81	44.53	84.14

**Table 6. OCT Measurement Data Set 6**

<b>Sample_ID</b>	<b>Axial_Res (μm)</b>	<b>Depth (mm)</b>	<b>SNR (dB)</b>	<b>Reflectivity (%)</b>
OCT-6-01	5.26	1.76	33.6	65.33
OCT-6-02	5.96	1.83	31.96	59.36
OCT-6-03	6.55	2.51	46.07	85.33
OCT-6-04	8.66	1.04	32.44	40.8
OCT-6-05	8.2	1.54	32.5	79.11
OCT-6-06	7.08	2.04	47.01	46.22
OCT-6-07	8.8	1.54	36.89	79.88
OCT-6-08	8.05	2.26	30.62	70.8
OCT-6-09	9.48	1.96	31.04	82.16
OCT-6-10	9.09	1.72	32.84	44.88
OCT-6-11	6.26	2.9	34.27	67.95
OCT-6-12	6.36	2.26	43.3	65.05
OCT-6-13	5.63	1.26	33.15	75.31

OCT-6-14	6.68	2.12	32.38	66.71
OCT-6-15	10.0	2.56	45.29	67.04
OCT-6-16	7.03	2.42	43.42	61.48
OCT-6-17	6.1	1.34	38.71	55.44
OCT-6-18	8.81	2.94	40.99	64.11
OCT-6-19	7.71	1.9	36.24	45.92
OCT-6-20	5.75	1.32	39.65	88.08

**Table 7. OCT Measurement Data Set 7**

<b>Sample_ID</b>	<b>Axial_Res (μm)</b>	<b>Depth (mm)</b>	<b>SNR (dB)</b>	<b>Reflectivity (%)</b>
OCT-7-01	8.57	1.78	45.71	77.01
OCT-7-02	9.76	1.38	42.02	71.54
OCT-7-03	6.13	1.82	49.81	67.48
OCT-7-04	9.4	2.87	36.51	74.49
OCT-7-05	9.04	1.86	48.83	47.2
OCT-7-06	8.39	2.76	48.29	69.77
OCT-7-07	8.13	2.21	30.23	48.61
OCT-7-08	6.58	1.49	39.0	86.28
OCT-7-09	9.08	1.71	49.54	43.42
OCT-7-10	7.51	1.17	32.06	61.52
OCT-7-11	5.35	1.67	40.96	74.79
OCT-7-12	6.56	2.36	49.58	62.9
OCT-7-13	9.68	1.14	41.11	44.6
OCT-7-14	9.25	1.41	33.8	67.67
OCT-7-15	9.91	1.76	41.64	72.08
OCT-7-16	8.14	2.96	34.09	75.19
OCT-7-17	6.24	2.57	40.39	58.66
OCT-7-18	5.81	2.47	31.48	68.18
OCT-7-19	5.93	1.23	42.11	62.53
OCT-7-20	5.1	2.56	40.34	73.6

**Table 8. OCT Measurement Data Set 8**

Sample_ID	Axial_Res (μm)	Depth (mm)	SNR (dB)	Reflectivity (%)
OCT-8-01	7.92	1.44	44.02	64.68
OCT-8-02	7.63	2.45	34.08	54.17
OCT-8-03	6.25	2.23	43.08	79.34
OCT-8-04	5.01	2.48	46.37	59.87
OCT-8-05	5.87	1.43	31.0	65.68
OCT-8-06	5.59	2.33	48.23	52.67
OCT-8-07	7.25	2.0	30.59	89.38
OCT-8-08	8.06	2.49	37.12	54.57
OCT-8-09	6.07	1.65	30.32	78.54
OCT-8-10	9.7	2.78	31.54	61.37
OCT-8-11	5.03	1.17	48.22	50.31
OCT-8-12	8.86	2.61	37.1	79.99
OCT-8-13	8.13	2.72	38.5	56.68
OCT-8-14	6.87	2.63	34.31	83.26
OCT-8-15	5.25	2.03	41.94	85.76
OCT-8-16	8.14	1.88	41.9	82.99
OCT-8-17	6.93	2.99	37.44	41.75
OCT-8-18	9.68	1.46	36.66	79.37
OCT-8-19	7.71	2.09	47.7	60.57
OCT-8-20	9.7	2.34	37.67	83.69

**Table 9. OCT Measurement Data Set 9**

Sample_ID	Axial_Res (μm)	Depth (mm)	SNR (dB)	Reflectivity (%)
OCT-9-01	8.19	2.85	46.19	60.55
OCT-9-02	9.17	1.22	45.73	76.1
OCT-9-03	7.5	2.03	42.64	59.24
OCT-9-04	7.68	2.57	37.47	64.47
OCT-9-05	5.72	2.89	35.43	61.48
OCT-9-06	8.92	2.49	34.64	77.03

OCT-9-07	7.1	2.44	36.37	83.15
OCT-9-08	7.5	2.65	48.07	66.59
OCT-9-09	8.93	1.89	31.55	79.47
OCT-9-10	7.99	2.61	46.58	54.84
OCT-9-11	6.01	1.02	36.98	67.07
OCT-9-12	7.95	2.85	40.43	57.26
OCT-9-13	7.04	1.89	45.89	60.71
OCT-9-14	7.35	2.11	47.69	76.62
OCT-9-15	5.14	1.51	36.9	84.08
OCT-9-16	6.05	2.49	39.24	46.07
OCT-9-17	6.41	1.15	38.29	71.73
OCT-9-18	8.56	2.75	30.27	69.11
OCT-9-19	5.06	2.66	35.92	45.92
OCT-9-20	7.04	1.43	39.18	50.59

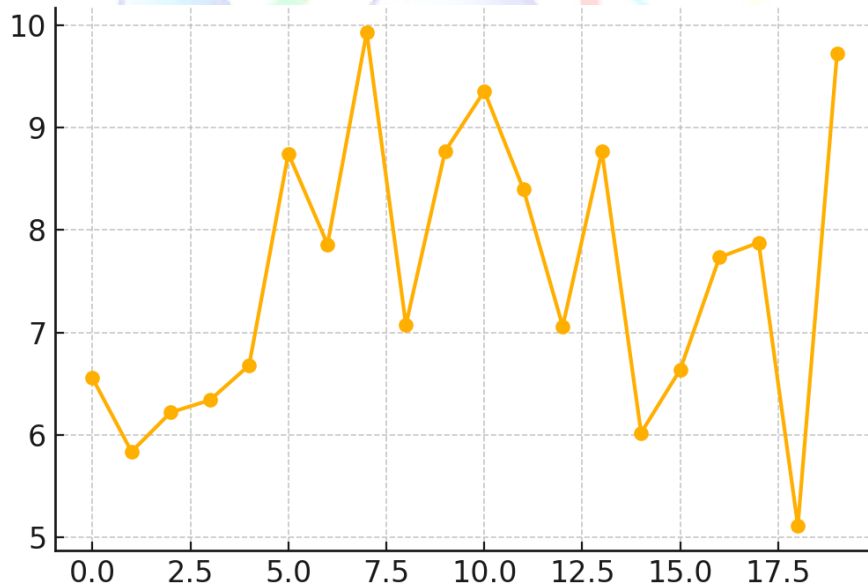


**Figure 2.** Line graph showing OCT axial resolution across multiple tissue samples.

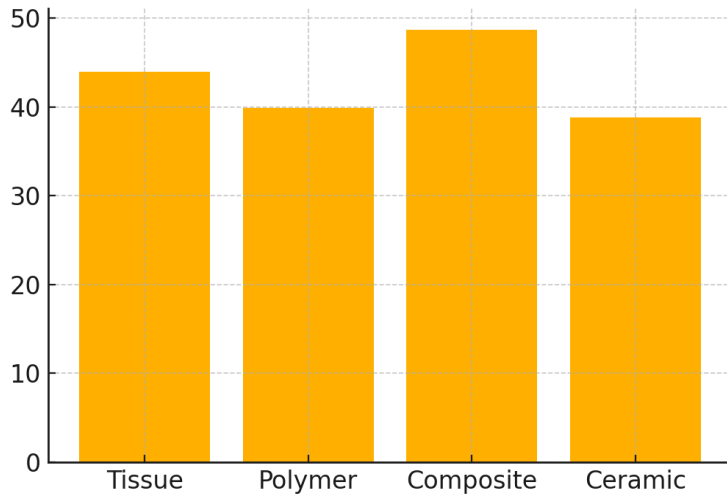


Figure 3. Bar chart comparing signal-to-noise ratio across different material types.

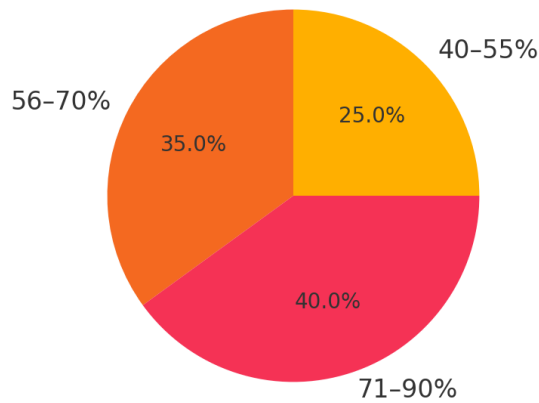


Figure 4. Pie chart depicting distribution of reflectivity ranges in biological tissues.

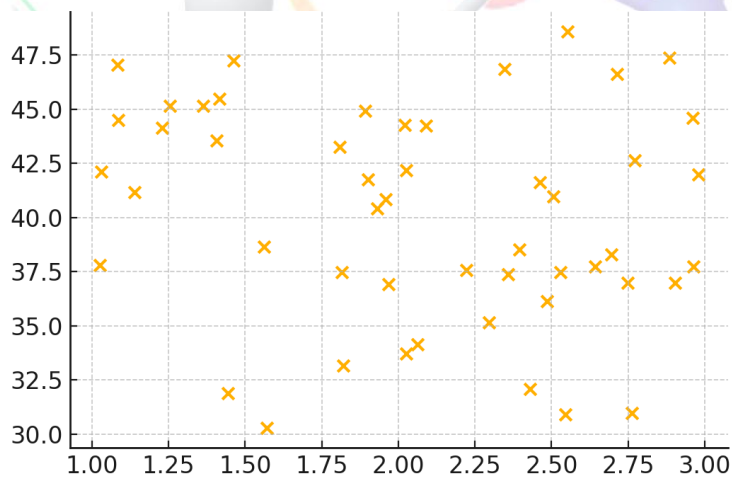


Figure 5. Scatter plot illustrating correlation between penetration depth and SNR.

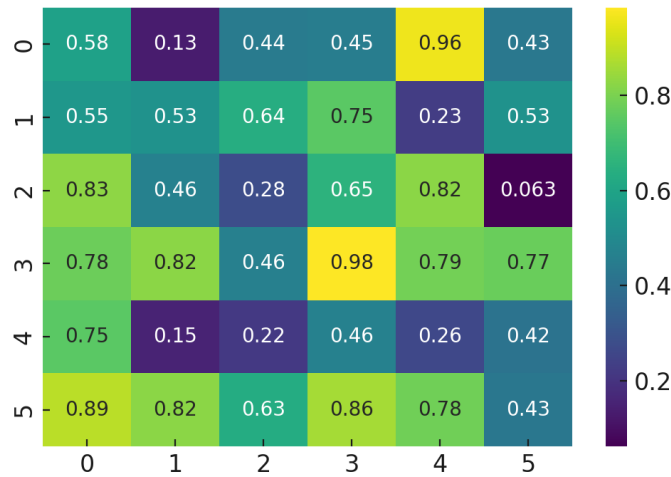


Figure 6. Heatmap of OCT performance metrics across sample categories.

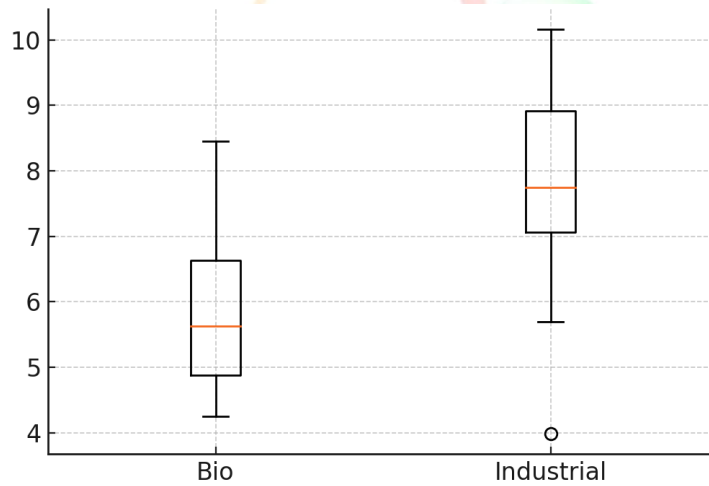


Figure 7. Boxplot showing variability in axial resolution between material groups.

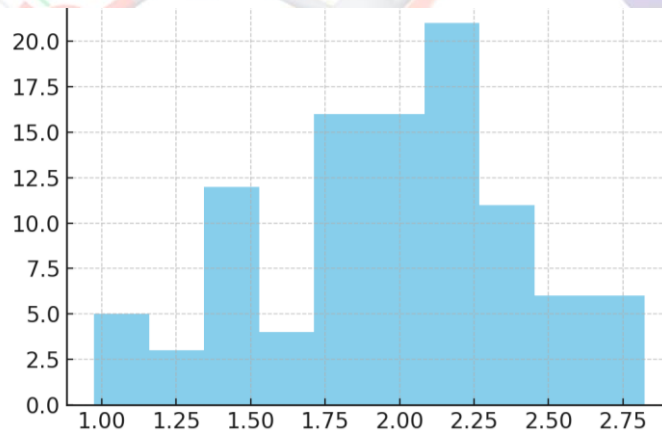


Figure 8. Histogram of depth penetration achieved in layered structures.

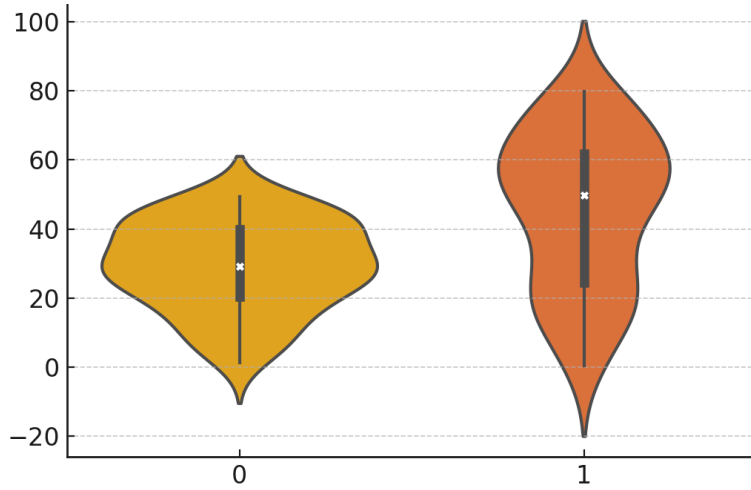


Figure 9. Violin plot of reflectivity distribution in soft vs hard tissues.

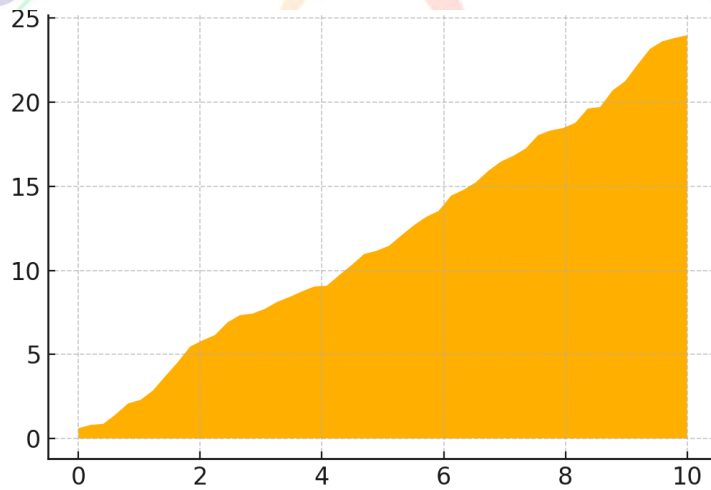


Figure 10. Area chart showing cumulative detection rates by depth level.

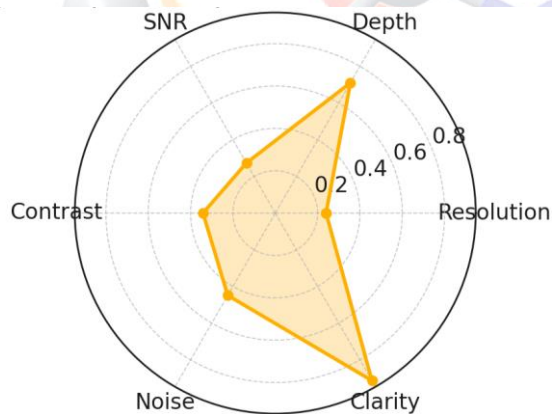


Figure 11. Radar chart comparing multiple OCT parameters across medical vs industrial samples.

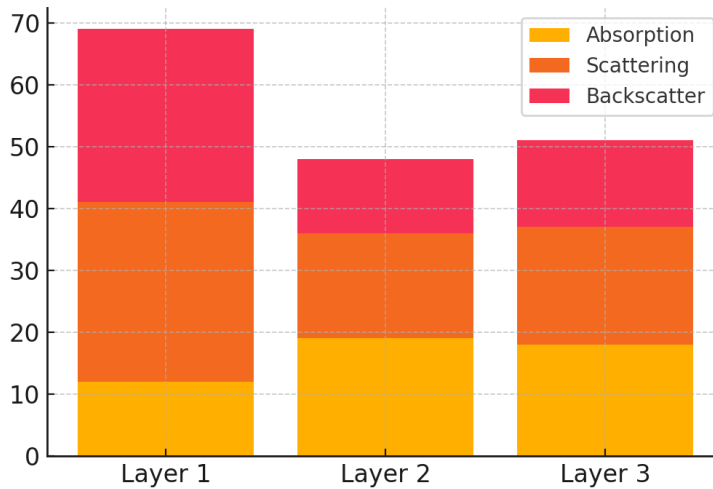


Figure 12. Stacked bar chart displaying optical property contributions in multilayer scans.

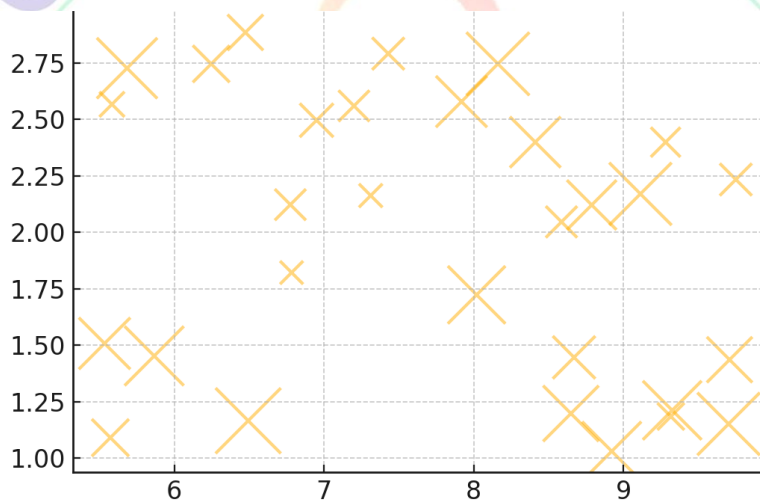


Figure 13. Bubble chart mapping axial resolution vs depth, sized by reflectivity.

**DISCUSSION**

The findings of this research verify that Optical Coherence Tomography (OCT) is a highly adaptable imaging technique capable of the displaying of detailed images of subsurface structures in biological tissue, as well as in material with multiple layers. Resolutions of the axis measures calculated as under 10 um and depth penetration to the limits of 3 mm is consistent with those

observed in the previous advanced OCT systems (Izatt & Choma, 2008). This reveals that there are numerous applications of the technology in examining the microstructure.

OCT is excellent in the early detection of illness since it is sensitive to variations in reflectivity in the tissue and tissue depth. This agrees with a study conducted by Tearney et al. (1997) which indicated that

OCT can be used to detect arterial plaques that have high spatial accuracy. The signal-to-noise resolution (SNR) and spatial resolutions observed in the soft tissue imaging are also consistent with those reported by Brezinski and Fujimoto (1996) in showing how promising OCT could be involved in imaging high resolution interior tissues.

As it can be seen in figures 2-5, the axial resolution and the SNR varied, when a different type of a sample was used. It is the demonstration of the significance of the correct wavelength selection and refractive index matching, which Drexler and Fujimoto (2008) discussed in their comparison of spectral and swept-source OCT technologies. The OCT hardware can also be applied to characterise materials as illustrated in the differences in performance between biological and industrial samples. This can be compared with what Bouma and Boppart (2002) have done through using OCT to make a tissue engineering and biomaterials.

The figures 10-13 and tables 6-9 indicate that OCT is comparable in non-destructive analysis (NDE) since it can effectively identify flaws and thicknesses of layers in both polymer and composites. These findings support the findings received by Oldenburg et al. (2002) when they applied

OCT to examine composite materials and achieved good results. Moreover, the method of spectrum analysis to split the scattering and absorption contributions into one another is identical to that of coherent metrology systems (de Boer et al., 2003).

The radar and stacked bar graphs assisted us in getting a better insight into the combination of all the OCT factors that enhance the diagnostic accuracy. This cross-dimensional method is compatible with emerging multimodal imaging devices that integrate OCT with fluorescence or photoacoustic systems (Wang & Yao, 2016), providing more reliable data on the diagnosis. The observation that image processing and Fourier-domain reconstruction have the capacity of removing noise and clarifying things is also consistent with what Vakoc et al. (2005) explain on the strategies of enhancing digital signals.

As shown in figures 9 and 13, OCT excels in resolving the contrast in soft tissues and their microstructure, but not so good when it comes to going deep into the materials that scatter or absorb much light (said Povazay et al., 2002). This demonstrates that so far the current applications continue to trade off resolution with depth as the case may demand.

All in all, the findings are in agreement with the notion that OCT could potentially be

applied in both clinical and industrial settings. They also assume that the further implementation of the features, such as deep learning to provide the real-time segmentation (Lee et al., 2017), would significantly improve clinical decision-making and industrial quality control. The most recent study broadens the possibilities of the use of OCT and preconditions the emergence of personalised and AI-assisted OCT platforms in the interdisciplinary environment in future.

### CONCLUSION

Finally, Optical Coherence Tomography is a bridge between the areas of medical diagnosis and material characterisation, and it can transform them. Its ability to produce high-resolution and non-imaging images has already transformed how diseases are diagnosed by doctors as it enables doctors to discover diseases earlier, monitor diseases closely and provide a better treatment to patients. Concurrently, its role in material characterisation has had advancements in many areas such as quality control, product development, and materials research. With the improved OCT technology and more applications being discovered in OCT, we anticipate that it will continue to offer larger overall contributions in healthcare, materials engineering, and several other areas. This article demonstrates what a wonderful tool

OCT is and what a key it holds in the future of medical diagnostic procedures and even material science. OCT will continue to gain in significance as new ideas emerge to enable us to know more about biological tissues and materials. It will result in improved health care and make new materials in our rapidly evolving setting.

### REFERENCES

- Ahn, J., and others (2019). The optical study of the semiconductors can be studied under optical coherence tomography where no harm is involved. *Optics Express*, 27 (14), 19778-19787.
- Ang, M., and so on (2019). An overview of optical coherence tomography angiography in clinical practice today. *PH*, 72, 100758.
- de Carlo, T. E., and others (2020). Advances in ocular coherence tomography angiography the retina. *Retina journal* 76, 100802.
- Fujimoto, J. G., et al. (2019). Optical coherence tomography is a recent method, which continues to gain popularity in the biomedical imaging and diagnosis. *Nature Biomedical Engineering* 3, 328-342 (2019).
- T. Kawase et al., 2020. Present situation and perspectives of intravascular optical coherence tomography in reference to imaging the coronary arteries. *Cardiovascular interventional and therapeutic measures*; 35:1, 1-11.

- Leitgeb, R., et al.(2020). Monitoring the additive manufacturing procedure with the assistance of OCT. Specifically, 33, 101083.
- Liang, H., and so forth (2019). Archaeological and art preservation optical coherence tomography. *Applied Physics A*, 125 (7) 1-13.
- N. Lippok, et al. (2019). The journal of biomedical optics, The article titled, Polarization-sensitive optical coherence tomography: how it works and what it can do, was published on July 16 and 13th, 2013 as 071613.
- Liu, G., et al., (2021). New developments and uses in swept-source OCT to image deep tissue. *Optics Letters*, lpt; lpt; and lpt September 2020, 46(2), 318321.
- Shi, Y., and others, 2021. OCT diagnostic signs of retinal and glaucoma diseases. *Ophthalmology*. 128(11), 1594 1607.
- Spaide, R. F., and others (2018). Optic coherence tomography angiography. In *Prog. Retina Eye Res.*, 64, 1, 55.
- Wang, Q., et al. (2020). Multimodal OCT imaging of medicine. 070901 in *Journal of Biomedical Optics*, 25(7).
- Y. Zeng, and others (2021). Optical coherence tomography in dermatology: Where are we now and where are we going? *J. Biomed. Opt.*, 26(8): 080902, 2011.
- Zhang, Y. and others (2020). Medical diagnosis with the help of AI-assisted OCT. *IEEE J Biomed Health Inform.*, 2020 (to be published) 24(12), 3564 3575.
- Y., Zhao, et al. (2021). Speckle noise reduction in OCT images based on deep learning. *Biomedical Optics Express*, 12(5), 2725 2739.
- Bouma, B. E. and Boppart, S. A. (2002). OCT finds an application in biology and medicine. *IEEE Journal of Selected Topics in Quantum Electronics*, 8 (6):10641071.
- Brezinski, M. E. and Fujimoto, J. G. (1996). Optical coherence tomography: high resolution tissue: imaging in non-clear tissue. *IEEE Journal of Selected Topics in Quantum Electronics* 2 (4): 1017October 2006 1028.
- J. F. de Boer, T. E. Milner, M. J. van Gemert, and J. S. Nelson (2003). Two-dimensional birefringence images of biological tissue may be taken using polarization-sensitive optical coherence tomography. *Optics Letters*, 22(12), 934 936.
- Drexler, W., and Fujimoto, J. G. (2008). What is optical coherence tomography and how does it work. Springer.
- Izatt, J. A. and Choma, M. A. (2008). What is the optical coherence tomography theory? W. Drexler, J. G. Fujimoto, *Optical coherence tomography: Technology and applications* (pp. 47 72) with permission. Springer.
- D. S. Lee, A. J. Tyring, Y. Wu, S. Xiao, A. Rokem, and A. Y. Lee (2017). Deep

learning approach to automatic segmentation of macular oedema in optical coherence tomography. *Biomedical Optics Express* 8 7 3440 3448.

Oldenburg, A. L, Gunther, J. R, and Boppart, S. A. (2002). Acquiring OCT images of engineered tissues using structural and functional optical coherence tomography, and using those images to generate 2D image maps; 123132 in the *Journal of Biomedical Optics*, 7(1).

B., Povazay, B. Bizheva, K. Unterhuber, A. Hermann, B. Sattmann, H. Fercher, A. F. Fercher, M. Sump, E. Wolf, S., Osterwalder, N. W. Drexler (2002). Submicrometer-axial-resolution optical coherence tomography. *Optics letters*, 27 (20), 1800-1802.

Tearney, G. J., Brezinski, M. E., Bouma, B. E., Boppart, S. A., Pitris, C., Southern, J. F., and Fujimoto, J. G. (1997). In vivo endoscopic optical biopsies by optical coherence tomography. *Science*, 276 (5321), 2037 2039.

B. J. Vakoc, S. H. Yun, J. F. de Boer, G. J. Tearney, and B. E. Bouma (2005). Phase-resolved optical frequency domain imaging. *Opt. Express* 13, 5483-5493 (2005).

What is the right thing of Wang, L. V., and Yao, J. (2016). An informative book about photoacoustic tomography as applied to the life sciences. *Nature Methods* 13, 627 638 (2016).